Original Article

Biomechanical properties and histomorphometric features of aortic tissue in patients with or without bicuspid aortic valve

Calogera Pisano[1#], Federico D'Amico[2#], Carmela Rita Balistreri[3], Sara Rita Vacirca[1], Paolo Nardi[1], Claudia Altieri[1], Maria Giovanna Scioli[2], Fabio Bertoldo[1], Loredana Santo[4], Denise Bellisario[4], Marco Talice[5], Roberto Verzicco[4], Giovanni Ruvolo[1*], Augusto Orlandi[2,6*]

[1]Department of Cardiac Surgery, Tor Vergata University Hospital, Rome, Italy; [2]Anatomic Pathology, Department of Biomedicine and Prevention Tor Vergata University, Rome, Italy; [3]Department of Biomedicine, Neuroscience and Advanced Diagnostics (Bi.N.D.), University of Palermo, Palermo, Italy; [4]Department of Industrial Engineering, Tor Vergata University, Rome, Italy; [5]PMSQUARED Engineering, Cagliari, Italy; [6]Department of Biomedical Sciences, Catholic University Our Lady of Good Counsel, Tirana, Albania

Contributions: (I) Conception and design: C Pisano, F D'Amico, R Verzicco, G Ruvolo, A Orlandi ; (II) Administrative support: C Pisano, R Verzicco, G Ruvolo, A Orlandi; (III) Provision of study materials or patients: C Pisano, F D'Amico, CR Balistreri, SR Vacirca, P Nardi, C Altieri, MG Scioli, F Bertoldo, L Santo, D Bellisario, M Talice; (IV) Collection and assembly of data: None; (V) Data analysis and interpretation: C Pisano, F D'Amico, CR Balistreri, R Verzicco, G Ruvolo, A Orlandi; (VI) Manuscript writing: All authors; (VII) Final approval of manuscript: All authors.

[#]These authors contributed equally to this work.

[*]These authors contributed equally as last author.

Correspondence to: Calogera Pisano, MD, PhD. Tor Vergata University Hospital, Viale Oxford 81, 00133 Rome, Italy.
Email: lindapisano82@gmail.com.

Background: We sought to investigate and compare biomechanical properties and histomorphometric findings of thoracic ascending aorta aneurysm (TAA) tissue from patients with bicuspid aortic valve (BAV) and tricuspid aortic valve (TAV) in order to clarify mechanisms underlying differences in the clinical course.

Methods: Circumferential sections of TAA tissue in patients with BAV (BAV-TAA) and TAV (TAV-TAA) were obtained during surgery and used for biomechanical tests and histomorphometrical analysis.

Results: In BAV-TAA, we observed biomechanical higher peak stress and lower Young modulus values compared with TAV-TAA wall. The right lateral longitudinal region seemed to be the most fragile zone of the TAA wall. Mechanical stress-induced rupture of BAV-TAA tissue was sudden and uniform in all aortic wall layers, whereas a gradual and progressive aortic wall breakage was described in TAV-TAA. Histomorphometric analysis revealed higher amount of collagen but not elastin in BAV-TAA tunica media.

Conclusions: The higher deformability of BAV-TAA tissue supports the hypothesis that increased wall shear stress doesn't explain the increased risk of sudden onset of rupture and dissection; other mechanisms, likely related to alteration of specific genetic pathways and epigenetic signals, could be investigated to explain differences in aortic dissection and rupture in BAV patients.

Keywords: Bicuspid aortic valve (BAV); aortic wall; aortopathy; fluid dynamic analysis; elastic tissue fragmentation

Submitted Dec 06, 2019. Accepted for publication Feb 12, 2020.
doi: 10.21037/jtd.2020.03.122
View this article at: http://dx.doi.org/10.21037/jtd.2020.03.122

Introduction

A bicuspid aortic valve (BAV) is characterized by an aortic valve with two semilunar leaflets. BAV is the most common congenital cardiovascular malformation with a prevalence of 0.5% to 2%, and it affects males four times more than females (1). BAV may evolve in serious complications, which occur in about 33% of patients. Aortic dilatation is the most common consequence of BAV, which determines the onset of thoracic aortic aneurysms (TAA) (2). Compared with patients with tricuspid aortic valve (TAV), patients

with BAV have a higher progression rate of dilation (3,4), suggesting differences in the process of dilation of the thoracic aorta. TAA onset is a very complex process; in which both cellular and extracellular mechanisms are involved. These mechanisms converge in a multiple signaling pathways and result in the maladaptive remodeling of the vascular extracellular matrix (5). The two main theories explaining the phenomenon of aortopathy in BAV disease are the genetic and the hemodynamic hypothesis (6). According to the genetic theory, the presence of aortic wall fragility is a consequence of a common developmental defect involving the aortic valve and the aortic wall and the mutation in NOTCH1 gene the main pathway involved (7-11). This hypothesis is further supported by reporting altered molecular and/or metabolic characteristics in the aortic wall and valve leaflets in BAV and differences in elastic lamellae, with a loose attachment of vascular smooth muscle cells (VSMCs), and precocious apoptosis. According to the hemodynamic theory, the abnormal hemodynamic stress on the aortic wall induced by eccentric turbulent flow through the BAV leads to subsequent aortopathy. Although the hemodynamic theory was the first explanation for BAV aortopathy, the genetic theory has become increasingly popular over the last decade (12-16). However, the widespread belief that BAV disease is a congenital disorder of vascular connective tissue led to recommendations for a more aggressive treatment of the proximal aorta in patients with TAA, approaching aortic management for patients with Marfan Syndrome-related aortopathy (17). Nevertheless, the aggressive surgical strategy for the treatment of aneurismatic aortopathy in patients with BAV has been questioned by some authors (18). In order to improve information on TAA in patients with BAV (BAV-TAA) and to better address the issue of pathogenesis of BAV-associated aortopathy, we investigated biomechanical properties and histological features of BAV and TAV.

Methods

Our study received approval from local ethic committees (Protocol Title: 01-Aorta-2018; Protocol Number: 179/18) and all participants gave their informed consent. Data were encoded to ensure patient and control protection.

Population

We compared patients with TAA associated with or not with BAV, with no history of aortic dissection. Our study included 26 TAA patients, 12 of them with TAV-TAA and 14 patients with BAV-TAA. Patients were admitted at the Cardiac Surgery Unit of Tor Vergata University from July 2017 to December 2018 to perform surgical treatment of the ascending aorta TAA. At the admission, all patients with BAV-TAA had an aortic valve dysfunction (regurgitation or stenosis), instead only half of patients with TAV-TAA had aortic valve dysfunction. Patients with aortic valve dysfunction, usually, referred dispnea at the admission. Patients without aortic valve dysfunction where asymptomatic. Clinical data of the studied patients were collected from clinical charts. Diameter evaluation of ascending aorta was made both preoperatively and in the operating room by transthoracic echocardiography (TTE) and transesophageal echocardiography (TEE) estimations performed as follows: dimensions of aortic annulus, sinuses of Valsalva and proximal ascending aorta (above 2.5 cm of the sinotubular junction) were estimated in parasternal long axis; the ones of aortic arch was evaluated from suprasternal view. Echocardiography derived sizes were reported as internal diameter size. Color Doppler was used to assess the presence and severity of aortic regurgitation and stenosis (see *Figure S1*). Furthermore, aortic root and ascending aorta diameter sizes were carried out using helical computed tomography image analysis techniques (*Figure S2*). For surgical procedure of TAA, we used the criteria advocated in the *ESC/EACTS Guidelines 2017 on Heart Valve Diseases*. In particular, we considered the surgical approach for those patients with a maximal ascending aortic diameter ≥50 mm in the presence of BAV and ≥55 mm in the presence of TAV. In addition, according our experience we considered surgery in presence of specific anatomical abnormality of aortic root unless the diameter: Valsalva sinus prolapse, thin and weak aortic wall with graining. Finally, when surgery was primary indicated for the aortic valve, replacement of the aortic root or tubular ascending aorta was considered when ≥45 mm, especially in the presence of BAV. The mostly used surgical procedures were isolated ascending aorta replacement or the button Bentall operation, which is a modification of the original technique described by Kouchoukos *et al.* 1991 (19). All the operations were performed using crystalloid or blood cardioplegia.

Biomechanical characterization

The mechanical properties of the aortic tissues were measured by tensile tests performed by the system MTS Insight 5 equipped by a load cell of 100 N. This

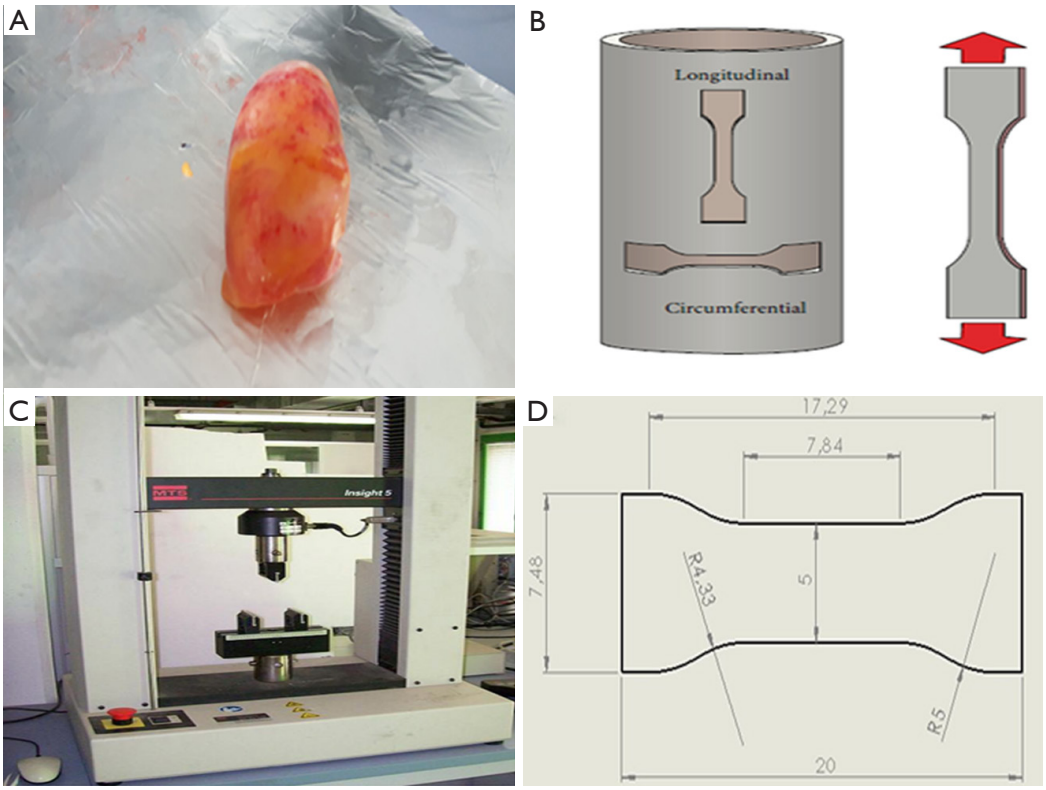

Figure 1 Biomechanical characterization. (A) Surgical aorta segment; (B) schematic description of segmental analysis of the aorta in the two directions; (C) MTS Insight Testing System (MTS System Corporation) used for the mechanical tests; (D) schematic description of the dimensions of each individual specimen.

device allows the tensile tests of virtually any material by prescribing the stretching force, the crosshead velocity (possibly time dependent) and the time evolution of the cycle, all desired features for the testing of biological materials.

Tissue specimens were extracted from the explanted aortic tract according to prescribed dimensions and shapes. Being the specimen dimensions fixed, the only variable dimension is the thickness of the tissue (S_0) that depends on the specific aortic sample and on the position of extraction (*Figure 1*).

Most of the biological tissues have a viscoelastic nature therefore, before proceeding to the material characterization, a preliminary preconditioning phase consisting of ten stretching cycles with a force in the range F_{min}=0.1 N and F_{max}=0.5 N is performed. This action aims at eliminating the initial transient behavior of the tissue so that its cycle-independent features can be measured. According to previous experiences, four cycles were enough to attain the final regime for human samples. It was decided anyway to precondition all samples with 10 cycles in order to be sure that every test had been performed under identical conditions. Immediately after the preconditioning, the final tensile test was performed with a constant crosshead velocity V=10 mm/min up to the rupture of the specimen. During this phase, data were collected in the form crosshead (mm) versus force (N) and successively processed to extract the relevant quantities. We considered L_0 and S_0 as the initial specimen length and thickness and A_0 as the initial minimum cross section area. Upon applying a stretching force F a length variation ΔL of the specimen was obtained and quantified by the stress $\sigma_e=F/A_0$ and the deformation $\varepsilon_e=\Delta L/L_0$. It must be noted, however, that as the specimen is stretched the length increases and its thickness decreases owing to volume conservation. If A, L and s are, respectively, the actual cross-sectional area, length and thickness of the specimen under tensile stretching, the volume conservation yields $A^*s = A_0^*S_0$ from which the actual stress can be computed as $\sigma=\sigma_e(1+\varepsilon_e)$ while the actual deformation is $\varepsilon=\ln(1+\varepsilon_e)$. All the cases have been analysed

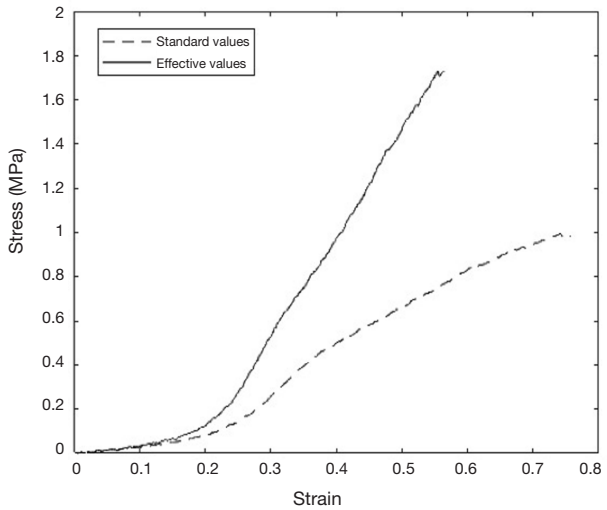

Figure 2 Example of traction curve: standard values and effective values.

by reporting σ versus ε obtaining curves as in *Figure 2* from which the peak stress (in MPa), i.e., the maximum stress achieved before specimen rupture, and the first Young Modulus (in MPa), which is the slope of the curve in the first linear part (20-24), have been obtained.

Hemodynamic simulations

Hemodynamic simulations have been performed using a finite volume, cell centered, computational fluid dynamics (CFD) code (IB-raptor, developed by PMSQUARED Engineering). The software is based on a semi-automatic decomposition of the fluid volume into small elements for which a discretized form of mass, momentum and energy conservation is applied. The Immersed Boundary (IB) method, which allows an efficient handling of complex geometries while retaining the accuracy of the solution is adopted. Another advantage of this CFD tool is that it can use the triangulated geometries directly obtained by the CT-scan of the patients. The fluid model for these simulations is Newtonian since the non-Newtonian blood features are known to be relevant only in sub-millimeter vessels; the kinematic viscosity of the blood has been assumed therefore constant and equal to $\nu=3.8\times10^{-6}$ N/m^2. A second order upwind scheme has been used for spatial discretization and an implicit Gauss-Seidel method for advancing in time to a steady state solution. A typical simulation is performed on a mesh containing one million of discrete elements whose dimensions are of the order of 0.1 mm next to the aortic wall and about 0.5 mm in the bulk of the flow. This difference is necessary in order to achieve enough spatial resolution for the accurate wall shear stress evaluation while keeping the computational load at an acceptable level. Such simulations take 4–8 hours on a parallel computer with four Intel i7 processors and generate solutions consisting of three-dimensional fields velocity, pressure and wall shear stress that can be reported and analysed through volume and surface renderings as in *Figure 3*.

Morphological and histomorphometric analysis

Serial 4-μm thick paraffin sections from 10% neutral-buffered formalin-fixed aortic tissue samples were stained with Haematoxylin&Eosin for microscopic examination or used for histochemical studies (25). Sections were stained with Alcian blue and Verhoeff-Van Gieson and extracellular accumulation of glycosaminoglycans (GAGs) and loss and fragmentation of elastic fibers were evaluated as reported (26,27). As control, we collected and analyzed autoptic thoracic aorta tissue samples (n=6) from patients (mean age =65.8 years) died for non-cardiovascular diseases (pulmonary and cerebral edema) to obtain healthy aorta samples. Moreover, Masson's trichrome-staining was performed to assess the collagen and elastic composition of the meshes and possible changes over the time after implantation. Masson's trichrome-staining intensity was arbitrarily scored on a scale of four grades: 0= negative, 1= weak positivity, 2= moderate positivity, 3= strong positivity (28).

Immunohistochemistry analysis

For immunohistochemistry, sections were reacted with rabbit polyclonal anti-metalloproteinases-2 (MMP-2, 1:750; Thermo Scientific Pierce, IL, USA, P1-16667). MMP-2 staining intensity was arbitrarily scored on a scale of four grades: 0= negative, 1= weak positivity, 2= moderate positivity, 3= strong positivity. Immunostainings were performed with positive and negative controls (29).

Statistical analysis

All blinded measurements were performed by two independent researchers, with an interobserved reproducibility >95%. Demographic and clinical analyses were performed with STATA 14.1 software. Histomorphometric and biomechanical analyses were

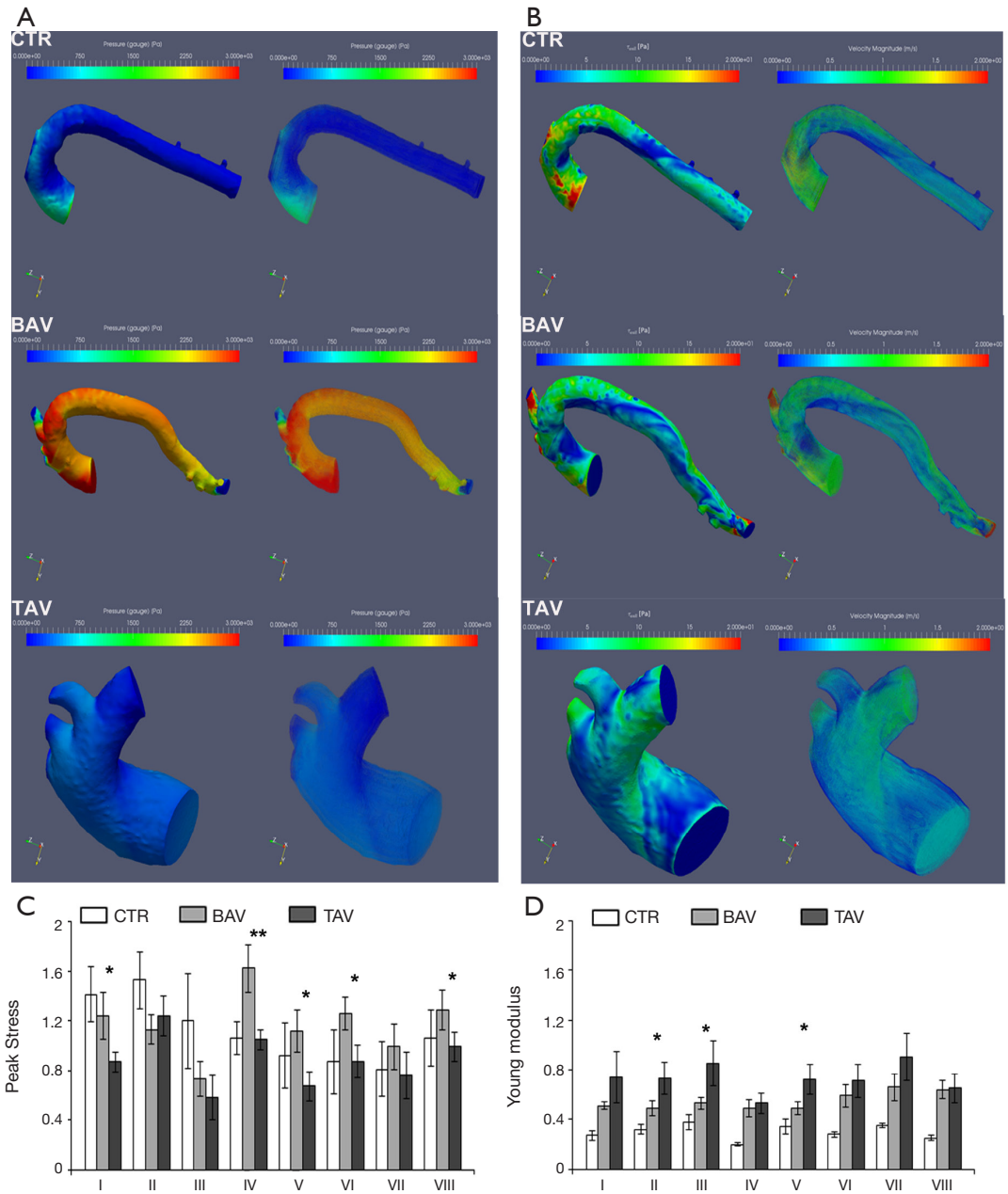

Figure 3 Hemodynamic simulations. (A) Pressure distribution (left) and fluid volume (right) on the aortic wall in a control, bicuspid and tricuspid aorta; (B) distribution of shear stress on the aortic wall (left) and fluid volume velocity (right) in a control, bicuspid and tricuspid aorta; (C) representative bar graphs of peak stress in BAV and TAV; (D) representative bar graphs of Young modulus in BAV and TAV. *t*-test: * and **, P<0.05 and P<0.01, respectively. I: anterior longitudinal region; II: anterior circumferential region; III: posterior longitudinal region; IV: posterior circumferential region; V: left lateral longitudinal region; VI: left lateral circumferential region; VII: right lateral longitudinal region; VIII: right lateral circumferential region. CTR, control aorta; BAV, bicuspid aortic valve; TAV, tricuspid aortic valve.

Table 1 Demographic and clinical characteristics of study population

Variables	BAV (n=14)	TAV (n=12)	P value
Gender, male	10 (71.4%)	7 (58.3%)	0.683
Age	62 [36–70]	76.5 [54–79]	0.001
BSA	2 (0.1)	1.9 (0.2)	0.410
BMI	28.2 (3)	27 (3)	0.332
Smoke	13 (68.4%)	10 (83.3%)	0,628
Hypertension	14 (73.6%)	9 (75%)	0.438
Preoperative echocardiographic parameters			
Aortic root	42 (9.01)	41.2 (5.6)	0.784
Ascending aorta	47.6 (5.3)	50.8 (6.1)	0.032
LVTDD	55 (6.2)	53 (7.7)	0.472
LVTSD	35.9 (4.8)	36.5 (6)	0.764
Septum	13 (1.4)	11.6 (1.6)	0.023
PP	12.5 (1.2)	11.8 (1.9)	0.283
LVTDV	120 (28.7)	116 (24.3)	0.708
LVTDV	50 [20–130]	50 [30–70]	0.306
EF	60 [47–65]	55 [20–60]	0.254
Mitral valve regurgitation	2 (14.2%)	2 (16.6%)	1.000
Aortic stenosis	7 (50%)	0 (0%)	0.006
Aortic regurgitation	12 (85.7%)	6 (50%)	0.090
PASP	35 [25,35]	35 [25,52]	0.302
Operative characteristics			
Procedure type			0.012
Bentall	14 (100%)	7 (58.3%)	
Ascending aorta replacement	0 (0%)	5 (41.6%)	
Cross clamp time	99.8 (26.8)	90.9 (33.4)	0.460
Cardioplegia			
Custodiol	3 (21.4%)	1 (8.3%)	0.598
Ematica	0 (0%)	1 (8.3%)	
St. Thomas	11 (78.5%)	10 (83.3%)	
Surgery time	240.5 [166–330]	206 [164–296]	0.180
Post operative characteristics			
Bleeding	2 (14.2%)	1 (8.3%)	1.000
Low cardiac output	0 (0%)	2 (16.6%)	0.203
Pace maker implantation	2 (14.2%)	2 (16.6%)	1.000
Post operative myocardial infarction	0 (0%)	2 (16.6%)	0.203
Pulmonary complications	2 (14.2%)	0 (0%)	0.483
Renal failure	2 (14.2%)	0 (0%)	0.483
Hospital mortality	0	0	–

LVTDD, left ventricular telediastolic diameter; LVTSD, left ventricular telesystolic diameter; LVTDV, left ventricular telesystolic volume; LVTSV, left ventricular telesystolic volume; EF, ejection fraction; PASP, pulmonary artery systolic pressure.

performed using SPSS 22 software (IBM SPSS Statistics). All categorical variables were reported as frequencies and percentages, while quantitative variables were synthesized as mean and standard deviation or standard error mean (SEM), minimum and maximum. The Fisher test for qualitative variables and the Kruskal-Wallis test or the one-way ANOVA technique for quantitative variables were used. The hypotheses of normality and homoscedasticity were verified through the Shapiro-Wilk test and the Fisher test. All the tests were considered significant for relative values $P<0.05$. Furthermore, odds ratios (OR) with 95% confidence intervals (CI) and their significance were calculated. Association between histological parameters and wall shear stress (WSS) was evaluated by using Pearson test. Statistical analyses were performed using SPSS 22 software (IBM SPSS Statistics).

Results

Characteristics of study population

All demographic variables, echocardiographic parameter, operative and postoperative characteristics were summarized in *Table 1*. The mean age in TAV patients was 76.5 [54–79] years and 62 [36–70] years in BAV patients (P value =0.001). The mean BMI in TAV patients was 28.2±3 and 25.8±2.5 in BAV patients. There were not statistical differences in term of hypertension and smoking between TAV and BAV patients. Sinus of Valsalva mean size was 41.2±6 mm in TAV patients and 42±9.01 mm in BAV patients (P value =0.332). Aneurysmatic ascending aorta mean size was 50.8 (6.1) mm in TAV patients and 47.6 (5.3) mm in BAV patients (P value =0.032). A Bentall de

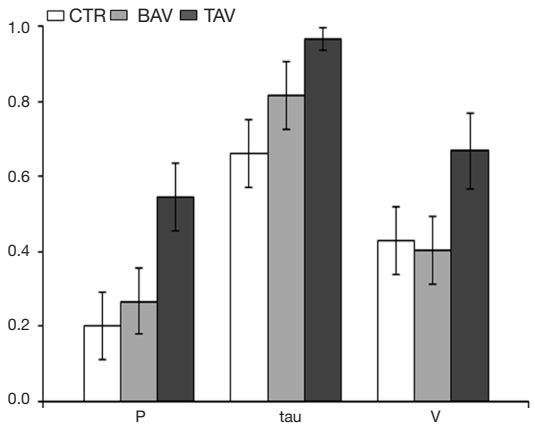

Figure 4 Representative bar graph of the root mean square (RMS) of pressure, wall shear stress and velocity fluctuations that quantify the smoothness of the flow. CTR, control aorta; BAV, bicuspid aortic valve; TAV, tricuspid aortic valve; P, pressure on the aorta wall; tau, wall shear stress; V, velocity fluctuations.

Bono operation was performed in all BAV patients and in 7 TAV patients; in the remaining 5 TAV patients an isolated ascending aorta replacement was performed. No statistical difference was observed in term of postoperative mortality and morbidity, including bleeding, permanent and transient brain injury, low cardiac output, pace-maker implantation, post-operative myocardial infarction, pulmonary failure requiring prolonged mechanical ventilation (>48 hours) and renal failure requiring dialysis.

Biomechanical properties

The biomechanical test showed that the value of peak stress before the aortic wall rupture was higher in BAV-TAA than in TAV-TAA tissue (see *Figure 3A,B,C*—V, VI, VII portions P<0.05, and IV portion P<0.01, respectively). The Young modulus value was lower in BAV-TAA than in TAV-TAA tissue (see *Figure 3D*—II, III, V portions P<0.05, respectively). In both BAV and in TAV patients, the right lateral longitudinal region of the TAA wall showed lowest value of peak stress before rupture and the highest value of Young modulus. TAA wall rupture was different between TAV-TAA and BAV-TAA (*Figure S3*). In BAV patients, the rupture of the aortic wall was sudden and involved uniformly all aortic wall layers, whereas in that from TAV patients a gradual and progressive aortic wall breakage was observed. Owing to the large computational cost of the hemodynamic simulations, a CFD analysis for each of the cases considered above has not been possible. Nevertheless, in order to assess the different flow features and a possible relation with the mechanical properties, one case for every patient category (BAV, TAV and CTR control) has been analysed and the results reported in *Figure 3*. Although these volume and surface renderings give an overall impression of the flow topology, they are not suitable to extract quantitative information and, for this reason, we have computed the mean value of the root mean square (RMS) of pressure, wall shear stress and velocity fluctuations that quantify the smoothness of the flow. The values are normalized with the mean value of the same quantity so that a root mean square of say 0.3 implies an intensity of the fluctuations that is 30% of the mean value. The bar graph of *Figure 4* clearly shows that both the TAV and the BAV configurations have fluctuation levels higher than for the control case. In particular, it is true for the wall shear stress and, in the long term, the anomalous stress fluctuation might be responsible for a remodelling of the tissues that, in turn, is evidenced by the different mechanical properties. In BAV patients the pressure, wall shear stress and velocity fluctuations were higher in the convexity of the ascending aorta and aortic arch. In TAV patients, there was a uniform distribution of the pressure, wall shear stress and velocity fluctuations.

Histomorphometric findings

Microscopic and histomorphometric examination of BAV and TAV aortic tissues did not show morphological characteristics or significant thickness variations (*Figure 5*). Microscopically, a variable diffuse medial thickening was present, with no differences in mean medial and intimal thickness between BAV, TAV TAA and control aortas. Semiquantitative evaluation of alcianophilia of the tunica media did not documented significant differences in GAG accumulation in TAA tissue of BAV and TAV groups, whereas control aortas showed lower GAGs accumulation (P<0.01). Verhoeff-Van Gieson staining showed increased fragmentation and reduced amount of elastic tissue in both BAV and TAV-TAA compared to control aorta (P<0.01 and P<0.05, respectively), with no differences between the two groups. Moreover, Masson's trichrome staining evidenced a different staining pattern in BAV compared with TAV group. In particular, TAV-TAA showed a significant increased density of collagen fibers compared to BAV-TAA (P<0.05).

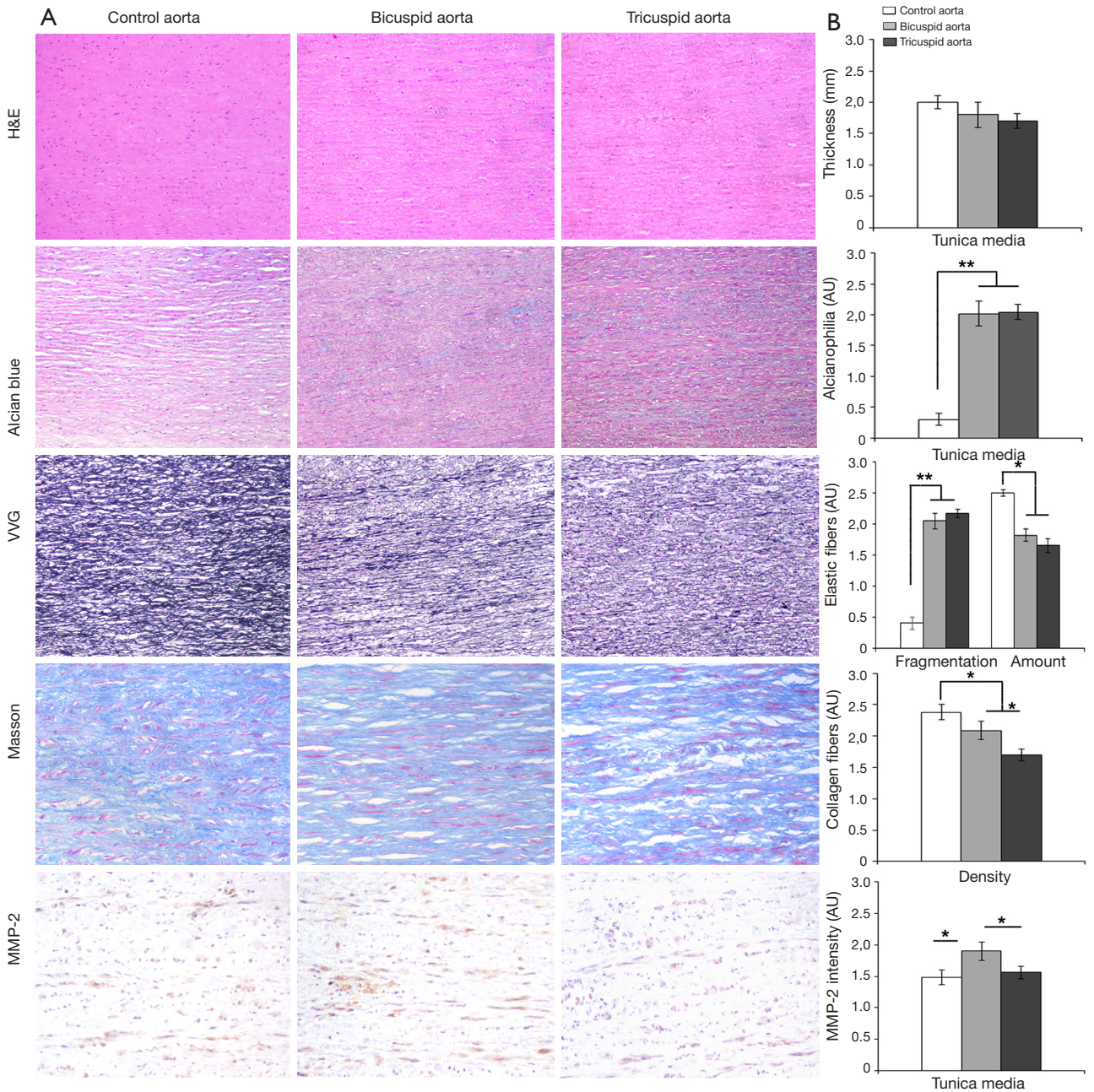

Figure 5 Microscopic and istomorphometric finding of aspects of human aortas in BAV and TAV aortopathy and in control aortic samples. (A) Aneurysmatic aortic tissue sections stained with Haematoxylin&Eosin showing medial degeneration with accumulation of basophilic material in BAV and TAV aortas. Alcian Blue staining shows accumulation of alcianophilic material in the tunica media of BAV, TAV and the control aortas. Verhoeff-Van Gieson staining documenting the loss and fragmentation of elastic fibers in the tunica media of a patient affected by BAV compared with the more regular arrangement of the tunica media in TAV aorta. Masson's trichrome staining showed a higher accumulation of collagen fibers in BAV compared with TAV group, instead in both groups collagen fibers were reduced compared with the control aortas. MMP-2 expression was increased in BAV compared to TAV and control groups. Original magnification, 100× and 200× for Masson's trichrome and MMP-2 staining; The magnification for VVG, Alcian blue, and H&E staining is 100×. (B) Representative bar graphs of Haematoxylin & Eosin, Alcian Blue, Verhoeff-Van Gieson, Masson's trichrome and MMP-2 staining in media tunic. *t*-test: * and **, P<0.05 and P<0.01, respectively. VVG, Verhoeff-Van Gieson; AU, arbitrary units; MMP-2, metalloproteinases-2.

Table 2 Correlation among histomorphometric findings and biomechanical properties

Groups	Peak stress *vs*. alcianophilia	Peak stress *vs*. elastic tissue fragmentation	Peak stress *vs*. tissue amount	Young modulus *vs*. alcianophilia	Young modulus *vs*. elastic tissue fragmentation	Young modulus *vs*. tissue amount
BAV						
I	–0.67*	–0.28**	0.29	–0.06	–0.28	0.29
II	–0.70**	–0.73***	0.29	–0.33	–0.21	0.13
III	–0.56	–0.40	0.34	0.32	0.12	0.25
IV	–0.90*	–0.88**	0.57	–0.04	–0.22	0.16
V	–0.66**	–0.69***	0.45	0.25	0.40	0.01
VI	–0.38*	0.02**	0.32	–0.04	0.13	–0.12
VII	–0.62**	–0.28**	0.32	–0.41	–0.03	–0.06
VIII	0.10**	0.35	0.35	–0.14	–0.17	0.25
TAV						
I	–0.12	0.52	–0.01	–0.13**	0.52***	–0.41
II	0.07**	–0.04**	–0.30	–0.21	0.70	–0.75
III	0.06	–0.19	0.28	0.28	0.58	–0.48
IV	0.21	0.02	–0.08	–0.24	0.71	–0.81
V	0.36	–0.37	0.02	0.01	0.62	–0.67
VI	–0.16	0.20	–0.16	–0.29	0.27	–0.09
VII	–0.08	0.36	–0.37	–0.19**	0.58***	–0.46
VIII	0.40	0.23	–0.40	–0.35	0.60	–0.80

I: anterior longitudinal region; II: anterior circumferential region; III: posterior longitudinal region; IV: posterior circumferential region; V: left lateral longitudinal region; IV: left lateral circumferential region; VII: right lateral longitudinal region; VIII: right lateral circumferential region. *t*-test: *, ** and ***, P<0.05, P<0.01 and P<0.001, respectively. Positive correlation: weak, 0<P<0.3; moderate, 0.3<P<0.7; strong, P>0.7. Negative correlation: weak, –0.3<P<0; moderate: –0.7<P<–0.3; strong: P<–0.7. BAV, bicuspid aortic valve; TAV, tricuspid aortic valve.

Immunohistochemical findings

Representative images of immunostaining for MMP-2 are reported in *Figure 5*. BAV-TAA showed an increased MMP-2 expression in the tunica media compared to other groups (P<0.05). MMP-2 medial expression in TAV-TAA was similar to that of control group.

Correlation between histomorphometric findings and biomechanical properties

Correlation analysis (*Table 2*) between histological parameters (alcianophilia, elastic tissue fragmentation and elastic tissue amount) and biomechanical properties (peak stress and Young modulus) revealed a moderate negative correlation between peak stress and alcianophilia in all BAV tissue portions (I and IV, P<0.05 and II, V, VII, P<0.01), except for the H portion, that displayed a weak positive correlation (P<0.01). The same moderate negative correlation was observed for the elastic fragmentation variable (I, IV and VII, P<0.01 and II and V, P<0.001), except for F portion displayed a weak positive correlation (P<0.01). Remaining correlations were almost weak and not significant (*Table 2*). Instead, correlation analysis in TAV group showed a weak positive correlation between peak stress and alcianophilia in II portion (P<0.01). The same was true for the correlation with the elastic fragmentation variable (II, P<0.01). Young modules and alcianophilia showed a significant weak negative correlation in I portion (P<0.01). Furthermore, Young modules value and elastic tissue fragmentation revealed a moderate positive correlation in A and G portions (P<0.001) (*Tables 2*,*3*).

Table 3 Summary of computational analysis of aorta, mechanical evaluation of aortic specimens and histology in patients with bicuspid aortic valve (BAV) and tricuspid aortic valve (TAV)

Type of aortic valve	Computational analysis	Biomechanical evaluation	Histomorphometrics and immunohistochemical findings
BAV	• Levels of fluctuation was high; • Flow velocity and pressure was higher in the convexity of the ascending aorta and aortic arch	• Before the aortic wall rupture the value of peak stress was higher in TAA tissue; • The Young modulus value was low in the aortic wall; • The right lateral longitudinal region of the TAA wall showed lowest value of peak stress before rupture and the highest value of Young modulus	• A variable diffuse medial thickening was present with no differences in mean medial and intimal thickness between groups; • Semiquantitative evaluation of alcianophilia of the tunica media documented similar accumulation of GAGs in TAA tissue between groups; • Verhoeff-Van Gieson staining showed increased fragmentation and reduced amount of elastic tissue; • Masson's trichrome staining showed a low density of collagen fibers; • Immunostaining for MMP-2 showed an increased expression in the aortic tunica media
TAV	• Levels of fluctuation was high; • There was a uniform distribution of flow velocity and pressure	• Before the aortic wall rupture the value of peak stress was lower in TAA tissue; • The Young modulus value was high in the aortic wall; • The right lateral longitudinal region of the TAA wall showed lowest value of peak stress before rupture and the highest value of Young modulus	• A variable diffuse medial thickening was present with no differences in mean medial and intimal thickness between groups; • Semiquantitative evaluation of alcianophilia of the tunica media documented similar accumulation of GAGs in TAA tissue between groups; • Verhoeff-Van Gieson staining showed increased fragmentation and reduced amount of elastic tissue; • Masson's trichrome staining showed a significant density of collagen fibers; • Immunostaining for MMP-2 showed a low expression in the aortic tunica media

Discussion

In the characterization of BAV aortopathy, flow dynamic is an emerging issue that induces dilation in the proximal aorta. This theory (hemodynamic theory) is supplanting the genetic hypothesis (6-8). Accordingly, several studies have reported that the differences in the phenotypes of BAV and in the type of valve dysfunction (stenosis versus regurgitation) result in distinct hemodynamics in the proximal aorta and influence strongly the risk for severe aortic events such as aortic rupture and dissection (30-37). To investigate how the hemodynamic turbulence induces aortic events, we investigated biomechanical properties and histological features of TAA tissue of BAV with those of TAV patients. Our histomorphometrical analysis reveled an increase of collagen content and MMP-2 expression in BAV-TAA compared to TAV-TAA wall. Biomechanical properties of ascending aorta largely depend on the composition and content of the extracellular matrix (38). The two main structural components responsible for aortic compliance are elastin and collagen, and their structural as well as functional modification may lead to altered mechanical properties, contributing to aortic dilatation and aneurysm development. Biomechanical prediction of vessel wall properties critically depends on realistic constitutive models of the aortic wall. *Ex vivo* tissue tests, together with mechanically histologic information provide valuable input to develop constitutive descriptions (39). Integrated microstructural information also helps to explore the mechanisms by which wall morphology and structure are linked to wall mechanics and allow testing the predictability of reported aortic adaptation models (40). According to our analysis, BAV-TAA showed a higher deformability and elasticity compared with TAV patients. Consequently, the increased wall shear stress according the hemodynamic theory could not explain the sudden onset of rupture and dissection in BAV patients. On the other hand, if BAV aorthopathy was a disease only caused by altered hemodynamics, the replacement of the malfunctioning BAV would subsequently not only cure the valvular disease but also prevent further dilatation of proximal aorta. Whereas this hypothesis was suggested to be partially true in stenotic BAVs (41), potentially representing the more flow-related type of BAV dysfunction, it appears allusive regarding regurgitant BAV. The more extended BAV aortopathy involving the

aortic root is associated with regurgitant BAV and remarkably, aortic dilatation and the risk of aortic events does not stagnate after aortic valve replacement but further progress (37,42). Additionally, Girdauskas *et al.* (43) reported that extensive aortic dilatation including the aortic root also occurred in a considerable amount of patients with only trace regurgitant BAV, indicating that hemodynamic stress is unlikely to explain this kind of BAV aortopathy, likely being more induced by a genetic pathways. Moreover, recent studies showed that epigenetic signals (non-coding RNAs, DNA methylation, histone modifications) and the alteration of microbiota are involved in vascular pathology of the thoracic ascending aorta associated with BAV (44,45). In our opinion, instead of considering hemodynamics and genetics as separate principles in the development of BAV aortopathy, the manifold phenotype of this disease could result rather from individually different impacts of both factors and their individual interaction. It is likely that wall shear stress activates specific genetic pathways in BAV patients affecting local extracellular matrix homeostasis and subsequently the phenotype of BAV aortopathy (43,46,47). This is a typical example of mechanotransduction trying to adapt to the altered force impact on the wall (48,49). According to this theory, we could also explain the different mechanism of rupture comparing TAA tissue from BAV and TAV patients. In particular, in BAV patients the rupture of the aortic wall was sudden and involved uniformly all the aortic wall layers, whereas in TAV patients there was a gradual and progressive aortic wall breakage. Our biomechanical and histomorphometric results have an important implication in the clinical field in term of surgical indication. In fact, since BAV patients display a higher susceptibility for rupture and dissection independently of the ascending aorta diameter and of the aortic wall shear stress, a more aggressive treatment recommendation of TAA is suggested in BAV patients. The main limitation to the present study is that small simple size, and an additional work is required to improve experiences to confirm our observations. The small simple size also made it impossible to evaluate the potential influence of valve disease on the observed results. Finally, cases of BAV-TAA cases were not enough to assess the flow dynamics related to the different BAV phenotypes according the fusion of the coronary cusps and the raphe position.

Conclusions

The TAA tissue of BAV patients showed a higher deformability compared with TAV patients. The increased wall shear stress according to the hemodynamic theory could not explain the sudden onset of rupture and dissection in BAV patients and other mechanisms, including the activation of specific genetic pathways, epigenetic signals and alteration of the microbiota, could be investigated to explain differences in aortic deformability and rupture in those patients. The recommendation of a more aggressive treatment of BAV-TAA is needed for the high resusceptibility for rupture and dissection independently of the ascending aorta diameter and of the shear stress.

Acknowledgments

The authors wish to thank Sabrina Cappelli for her technical assistance.
Funding: None.

Footnote

Conflicts of Interest: All authors have completed the ICMJE uniform disclosure form (available at http://dx.doi.org/10.21037/jtd.2020.03.122). The authors have no conflicts of interest to declare.

Ethical Statement: The authors are accountable for all aspects of the work in ensuring that questions related to the accuracy or integrity of any part of the work are appropriately investigated and resolved. Our study received approval from local ethic committees (Protocol Title: 01-Aorta-2018; Protocol Number: 179/18) and all participants gave their informed consent.

References

1. Siu SC, Silversides CK. Bicuspid aortic valve disease. J Am Coll Cardiol 2010;55:2789-800.
2. Yuan SM, Jing H, Lavee J. The bicuspid aortic valve and its relation to aortic dilation. Clinics (Sao Paulo) 2010;65:497-505.

3. Ferencik M, Pape LA. Changes in size of ascending aorta and aortic valve function with time in patients with congenitally bicuspid aortic valves. Am J Cardiol 2003;92:43-6.
4. Beroukhim RS, Kruzick TL, Taylor AL, et al. Progression of aortic dilation in children with a functionally normal bicuspid aortic valve. Am J Cardiol 2006;98:828-30.
5. Balistreri CR, Pisano C, Candore G, et al. Focus on the unique mechanisms involved in thoracic aortic aneurysm formation in bicuspid aortic valve versus tricuspid aortic valve patients: clinical implications of a pilot study. Eur J Cardiothorac Surg 2013;43:e180-6.
6. Girdauskas E, Borger MA, Secknus MA, et al. Is aortopathy in bicuspid aortic valve disease a congenital defect or a result of abnormal hemodynamics? A critical reappraisal of a one-sided argument. Eur J Cardiothorac Surg 2011;39:809-14.
7. Liu T, Xie M, Lv Q, et al. Bicuspid Aortic Valve: An Update in Morphology, Genetics, Biomarker, Complications, Imaging Diagnosis and Treatment. Front Physiol 2018;9:1921.
8. Niaz T, Hagler DJ. Is there a genetic basis to the different morphological subtypes of bicuspid aortic valve? Ann Transl Med 2018;6:S117.
9. Harrison OJ, Visan AC, Moorjani N, et al. Defective NOTCH signaling drives increased vascular smooth muscle cell apoptosis and contractile differentiation in bicuspid aortic valve aortopathy: A review of the evidence and future directions. Trends Cardiovasc Med 2019;29:61-8.
10. Miller RL, Diamonstein CJ, Benheim A. The importance of genetics and genetic counselors in the evaluation of patients with bicuspid aortic valve and aortopathy. Curr Opin Cardiol 2019;34:73-8.
11. Balistreri CR, Crapanzano F, Schirone L, et al. Deregulation of Notch1 pathway and circulating endothelial progenitor cell (EPC) number in patients with bicuspid aortic valve with and without ascending aorta aneurysm. Sci Rep 2018;8:13834.
12. Rose MJ, Rigsby CK, Berhane H, et al. 4-D flow MRI aortic 3-D hemodynamics and wall shear stress remain stable over short-term follow-up in pediatric and young adult patients with bicuspid aortic valve. Pediatr Radiol 2019;49:57-67.
13. Edlin J, Youssefi P, Bilkhu R, et al. Haemodynamic assessment of bicuspid aortic valve aortopathy: a systematic review of the current literature. Eur J Cardiothorac Surg 2019;55:610-7.
14. Liu J, Shar JA, Sucosky P. Wall Shear Stress Directional Abnormalities in BAV Aortas: Toward a New Hemodynamic Predictor of Aortopathy? Front Physiol 2018;9:993.
15. Bollache E, Guzzardi DG, Sattari S, et al. Aortic valve-mediated wall shear stress is heterogeneous and predicts regional aortic elastic fiber thinning in bicuspid aortic valve-associated aortopathy. J Thorac Cardiovasc Surg 2018;156:2112-20.e2.
16. Rodriguez-Palomares JF, Dux-Santoy L, Guala A, et al. Aortic flow patterns and wall shear stress maps by 4D-flow cardiovascular magnetic resonance in the assessment of aortic dilatation in bicuspid aortic valve disease. J Cardiovasc Magn Reson 2018;20:28.
17. Romaniello F, Mazzaglia D, Pellegrino A, et al. Aortopathy in Marfan syndrome: an update. Cardiovasc Pathol 2014;23:261-6.
18. Kaneko T, Shekar P, Ivkovic V, et al. Should the dilated ascending aorta be repaired at the time of bicuspid aortic valve replacement? Eur J Cardiothorac Surg 2018;53:560-8.
19. Kouchoukos NT, Wareing TH, Murphy SF, et al. Sixteen-year experience with aortic root replacement. Results of 172 operations. Ann Surg 1991;214:308-18; discussion 318-20.
20. Duprey A, Khanafer K, Schlicht M, et al. In vitro characterisation of physiological and maximum elastic modulus of ascending thoracic aortic aneurysms using uniaxial tensile testing. Eur J Vasc Endovasc Surg 2010;39:700-7.
21. Khanafer K, Duprey A, Zainal M, et al. Determination of the elastic modulus of ascending thoracic aortic aneurysm at different ranges of pressure using uniaxial tensile testing. J Thorac Cardiovasc Surg 2011;142:682-6.
22. Ferrara A, Morganti S, Totaro P, et al. Human dilated ascending aorta: Mechanical characterization via uniaxial tensile tests. J Mech Behav Biomed Mater 2016;53:257-71.
23. Okamoto RJ, Wagenseil JE, DeLong WR, et al. Mechanical properties of dilated human ascending aorta. Ann Biomed Eng 2002;30:624-35.
24. Charalambous HP, Roussis PC, Giannakopoulos AE. Viscoelastic dynamic arterial response. Comput Biol Med 2017;89:337-54.
25. Orlandi A, Pucci S, Ciucci A, et al. Modulation of clusterin isoforms is associated with all-trans retinoic acid-induced proliferative arrest and apoptosis of intimal smooth muscle cells. Arterioscler Thromb Vasc Biol 2005;25:348-53.
26. Orlandi A, Mauriello A, Marino B, et al. Age-related modifications of aorta and coronaries in the rabbit: a

morphological and morphometrical assessment. Arch Gerontol Geriatr 1993;17:37-53.
27. Orlandi A, Francesconi A, Marcellini M, et al. Role of ageing and coronary atherosclerosis in the development of cardiac fibrosis in the rabbit. Cardiovasc Res 2004;64:544-52.
28. Bernardini R, Varvaras D, D'Amico F, et al. Biological acellular pericardial mesh regulated tissue integration and remodeling in a rat model of breast prosthetic implantation. J Biomed Mater Res B Appl Biomater 2020;108:577-90.
29. Orlandi A, Ciucci A, Ferlosio A, et al. Increased expression and activity of matrix metalloproteinases characterize embolic cardiac myxomas. Am J Pathol 2005;166:1619-28.
30. Sievers HH, Schmidtke C. A classification system for the bicuspid aortic valve from 304 surgical specimens. J Thorac Cardiovasc Surg 2007;133:1226-33.
31. Sievers HH, Sievers HL. Aortopathy in bicuspid aortic valve disease - genes or hemodynamics? or Scylla and Charybdis? Eur J Cardiothorac Surg 2011;39:803-4.
32. Michelena HI, Khanna AD, Mahoney D, et al. Incidence of aortic complications in patients with bicuspid aortic valves. JAMA 2011;306:1104-12.
33. Della Corte A, Bancone C, Quarto C, et al. Predictors of ascending aortic dilatation with bicuspid aortic valve: a wide spectrum of disease expression. Eur J Cardiothorac Surg 2007;31:397-404; discussion 404-5.
34. Sievers HH, Stierle U, Hachmann RM, et al. New insights in the association between bicuspid aortic valve phenotype, aortic configuration and valve haemodynamics. Eur J Cardiothorac Surg 2016;49:439-46.
35. Girdauskas E, Rouman M, Disha K, et al. Morphologic and Functional Markers of Aortopathy in Patients With Bicuspid Aortic Valve Insufficiency Versus Stenosis. Ann Thorac Surg 2017;103:49-57.
36. Girdauskas E, Rouman M, Disha K, et al. Aortopathy in Bicuspid Aortic Valve Stenosis with Fusion of Right-Left versus Right-Non-Coronary Cusps: Are These Different Diseases? J Heart Valve Dis 2016;25:262-9.
37. Wang Y, Wu B, Li J, et al. Impact of Aortic Insufficiency on Ascending Aortic Dilatation and Adverse Aortic Events After Isolated Aortic Valve Replacement in Patients With a Bicuspid Aortic Valve. Ann Thorac Surg 2016;101:1707-14.
38. Michelena HI, Della Corte A, Prakash SK, et al. Bicuspid aortic valve aortopathy in adults: Incidence, etiology, and clinical significance. Int J Cardiol 2015;201:400-7.
39. Forsell C, Bjorck HM, Eriksson P, et al. Biomechanical properties of the thoracic aneurysmal wall: differences between bicuspid aortic valve and tricuspid aortic valve patients. Ann Thorac Surg 2014;98:65-71.
40. Lanir Y. Constitutive equations for fibrous connective tissues. J Biomech 1983;16:1-12.
41. Humphrey JD, Taylor CA. Intracranial and abdominal aortic aneurysms: similarities, differences, and need for a new class of computational models. Annu Rev Biomed Eng 2008;10:221-46.
42. Girdauskas E, Disha K, Borger MA, et al. Long-term prognosis of ascending aortic aneurysm after aortic valve replacement for bicuspid versus tricuspid aortic valve stenosis. J Thorac Cardiovasc Surg 2014;147:276-82.
43. Girdauskas E, Rouman M, Disha K, et al. Aortic Dissection After Previous Aortic Valve Replacement for Bicuspid Aortic Valve Disease. J Am Coll Cardiol 2015;66:1409-11.
44. Balistreri CR, Forte M, Greco E, et al. An overview of the molecular mechanisms underlying development and progression of bicuspid aortic valve disease. J Mol Cell Cardiol 2019;132:146-53.
45. Forte A, Balistreri CR, De Feo M, et al. Polyamines and microbiota in bicuspid and tricuspid aortic valve aortopathy. J Mol Cell Cardiol 2019;129:179-87.
46. den Reijer PM, Sallee D 3rd, van der Velden P, et al. Hemodynamic predictors of aortic dilatation in bicuspid aortic valve by velocity-encoded cardiovascular magnetic resonance. J Cardiovasc Magn Reson 2010;12:4.
47. Hope MD, Hope TA, Crook SE, et al. 4D flow CMR in assessment of valve-related ascending aortic disease. JACC Cardiovasc Imaging 2011;4:781-7.
48. Hope MD, Hope TA, Meadows AK, et al. Bicuspid aortic valve: four-dimensional MR evaluation of ascending aortic systolic flow patterns. Radiology 2010;255:53-61.
49. Hope MD, Sigovan M, Wrenn SJ, et al. MRI hemodynamic markers of progressive bicuspid aortic valve-related aortic disease. J Magn Reson Imaging 2014;40:140-5.

Cite this article as: Pisano C, D'Amico F, Balistreri CR, Vacirca SR, Nardi P, Altieri C, Scioli MG, Bertoldo F, Santo L, Bellisario D, Talice M, Verzicco R, Ruvolo G, Orlandi A. Biomechanical properties and histomorphometric features of aortic tissue in patients with or without bicuspid aortic valve. J Thorac Dis 2020;12(5):2304-2316. doi: 10.21037/jtd.2020.03.122

Supplementary

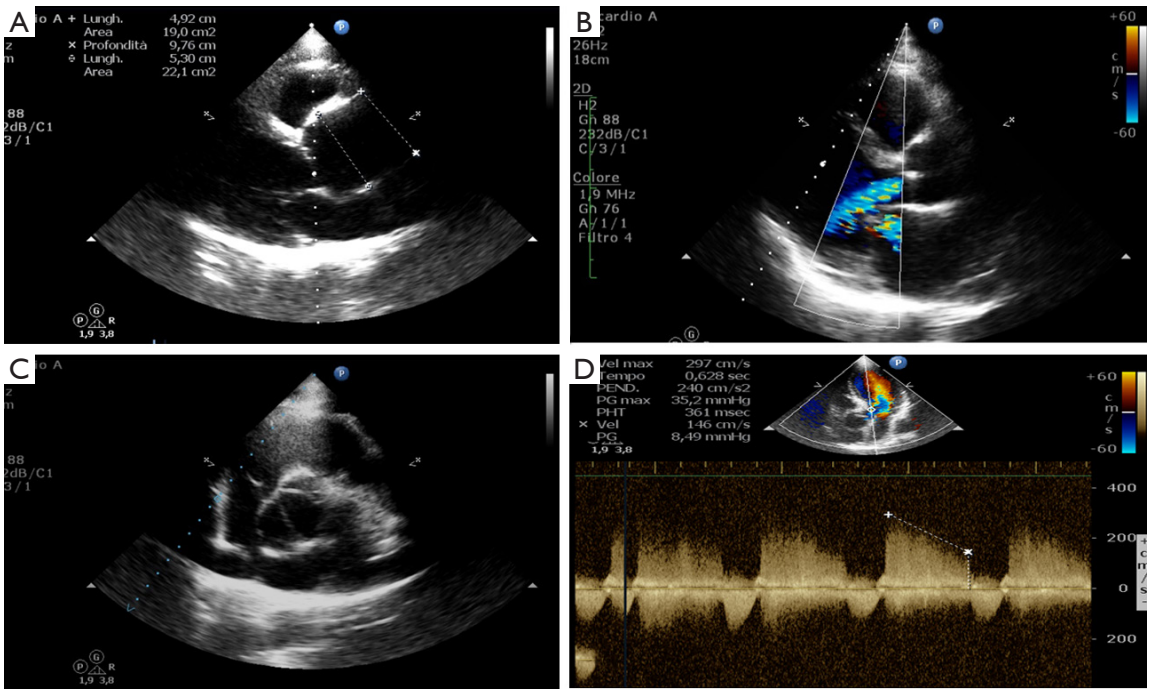

Figure S1 Transthoracic echocardiography examination: (A) ascending aorta aneurysm; (B) bicuspid aortic valve; (C) aortic valve regurgitation; (D) ecocolor Doppler evaluation.

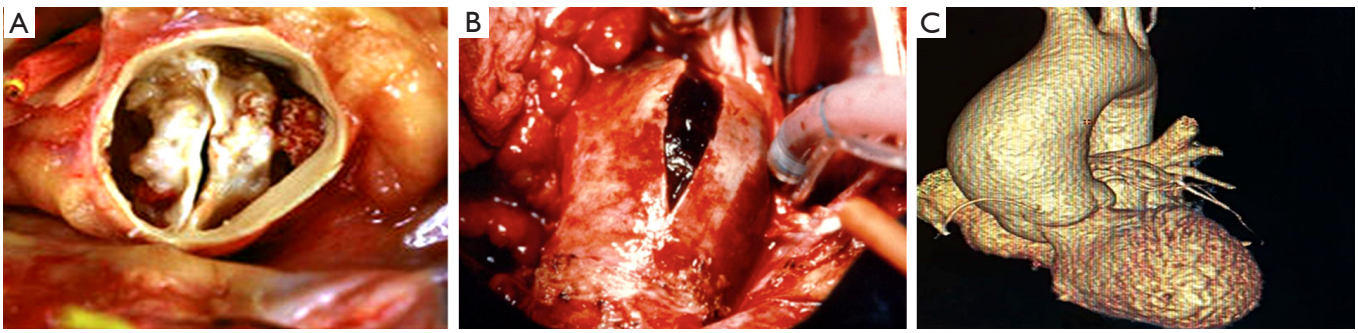

Figure S2 Ascending aorta aneurysm and bicuspid aortic valve. (A) Intraoperative view of bicuspid aortic valve (BAV); (B) intraoperative view of ascending aortic aneurysm associated to BAV; (C) computed tomography view of ascending aortic aneurysm.

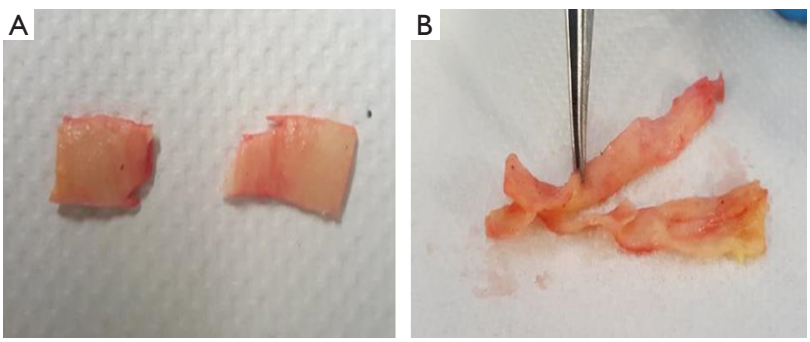

Figure S3 Ascending aorta specimens. (A) Uniform rupture of all layers of the aorta, found in the bicuspid aortic valve (BAV) group; (B) rupture with "flaking" of the aortic wall and progressive rupture of the three layers, found in the tricuspid aortic valve (TAV) group.